JACS
JOURNAL OF THE AMERICAN CHEMICAL SOCIETY

Article

pubs.acs.org/JACS

Phosphoryl Transfer by Protein Kinase A Is Captured in a Crystal Lattice

Adam C. Bastidas,[†] Michael S. Deal,[‡] Jon M. Steichen,[‡] Yurong Guo,[‡] Jian Wu,[‡] and Susan S. Taylor*[,†,‡,§]

[†]Department of Pharmacology, University of California, San Diego, California 92093, United States
[‡]Department of Chemistry and Biochemistry, University of California, San Diego, California 92093, United States
[§]Howard Hughes Medical Institute, University of California, San Diego, California 92093, United States

Supporting Information

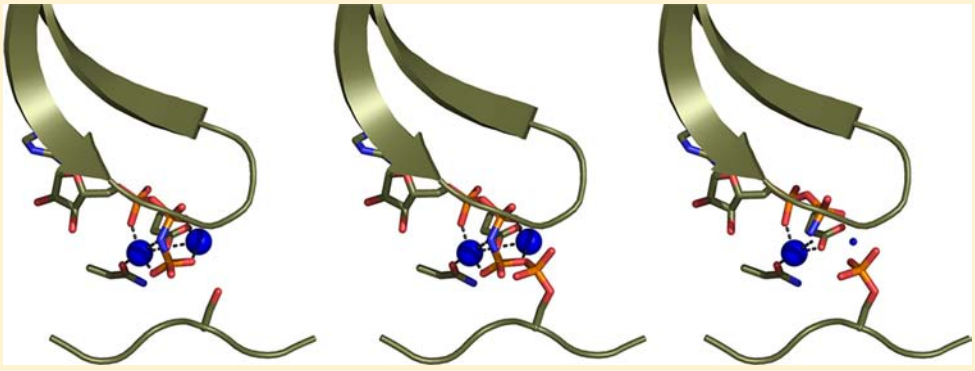

ABSTRACT: The catalytic (C) subunit of cAMP-dependent protein kinase (PKA) is a serine/threonine kinase responsible for most of the effects of cAMP signaling, and PKA serves as a prototype for the entire kinase family. Despite multiple studies of PKA, the steps involved in phosphoryl transfer, the roles of the catalytically essential magnesium ions, and the processes that govern the rate-limiting step of ADP release are unresolved. Here we identified conditions that yielded slow phosphoryl transfer of the γ-phosphate from the generally nonhydrolyzable analog of ATP, adenosine-5′-(β,γ-imido)triphosphate (AMP-PNP), onto a substrate peptide within protein crystals. By trapping both products in the crystal lattice, we now have a complete resolution profile of all the catalytic steps. One crystal structure refined to 1.55 Å resolution shows two states of the protein with 55% displaying intact AMP-PNP and an unphosphorylated substrate and 45% displaying transfer of the γ-phosphate of AMP-PNP onto the substrate peptide yielding AMP-PN and a phosphorylated substrate. Another structure refined to 2.15 Å resolution displays complete phosphoryl transfer to the substrate. These structures, in addition to trapping both products in the crystal lattice, implicate one magnesium ion, previously termed Mg2, as the more stably bound ion. Following phosphoryl transfer, Mg2 recruits a water molecule to retain an octahedral coordination geometry suggesting the strong binding character of this magnesium ion, and Mg2 remains in the active site following complete phosphoryl transfer while Mg1 is expelled. Loss of Mg1 may thus be an important part of the rate-limiting step of ADP release.

INTRODUCTION

One of the major mechanisms of cell signaling and gene regulation is protein phosphorylation. Phosphorylation is catalyzed by protein kinases, which transfer the γ-phosphate of ATP onto substrate proteins on serine, threonine, and tyrosine residues. Because of their roles in cancer and other diseases, kinases have become an important pharmaceutical target.[1] One of the best characterized protein kinases is the Ser/Thr kinase cAMP-dependent protein kinase (protein kinase A (PKA)), which serves as a prototype for the entire kinase family.[2−4] Under nonactivating conditions, PKA exists as a heterotetrameric holoenzyme complex composed of a regulatory (R) subunit dimer that binds to and inactivates two catalytic (C) subunit monomers (R_2C_2). PKA is activated by cAMP, which binds to the R-subunits causing a conformational change unleashing the active C-subunits, which can then phosphorylate protein substrates.[5]

The C-subunit of PKA was the first kinase structure to be solved[6] and has served as a prototype for protein kinases because of the multiple biophysical, structural, and computational studies of PKA.[7] PKA serves as a model for all kinases because the core of the enzyme, residues 40−300, is highly conserved. This conserved core forms a bean shaped structure consisting of the small lobe (or N-lobe) (residues 40−126 in PKA) and the large lobe (or C-lobe) (residues 127−300 in PKA). ATP binds in the cleft formed between these two lobes,[8] and recent NMR studies show how binding of the nucleotide

Received: December 18, 2012
Published: March 4, 2013

acts to dynamically couple the two lobes making it "committed" to catalysis.[9]

The precise mechanism of phosphoryl transfer and the detailed structural validation of the individual steps involved in catalysis are still not well understood for PKA or kinases in general. PKA, like most kinases, requires magnesium ions to catalyze phosphoryl transfer, and magnesium increases the affinity of the enzyme for ATP.[10] Other metals such as manganese can also be utilized by kinases *in vitro*,[8,11] but because of cellular concentrations, magnesium is thought to be the physiological metal cofactor. There are two magnesium binding sites in PKA.[8,12,13] One magnesium ion is coordinated by the β- and γ-phosphates of ATP, by Asp184 in a bidendate manner, and by two water molecules and was previously termed Mg1 and activating. The other magnesium ion is coordinated by Asn171, one oxygen atom of Asp184, the α- and γ-phosphates of ATP, and one water molecule and was termed Mg2 and inhibiting.[14,15] The active site water molecules that help to coordinate the magnesium ions were shown to be highly conserved among many protein kinases likely due to conservation of key active site residues.[16] The activating/inhibiting terminology used to describe the magnesium ions arises from the fact that low concentrations of magnesium (0.5 mM) yield higher $k_{cat.}$ values than high magnesium concentrations (10 mM) suggesting an inhibitory effect attributed to one of the two magnesium ions.[14,17,18] However, this terminology is slightly misleading because binding two magnesium ions does not actually influence the rate of phosphoryl transfer but, instead, affects the rate of ADP release which is the rate-limiting step at high magnesium concentrations.[14,17] The identity of Mg2 as the secondary and inhibitory ion may arise partially from an early report which suggested that low resolution structures obtained under low magnesium concentration displayed density mostly for Mg1 with very little density for Mg2.[15] Therefore, Mg1 was thought to bind first and with higher affinity with ATP and was thought to be the more important ion for phosphoryl transfer. With ADP, the two magnesium ions were thought to bind with equal affinity, which may explain why the ADP off rate limits turnover at higher magnesium concentration.[10] However, recently, another structure obtained under low magnesium concentration showed density for only Mg2.[19] Additionally, computational studies of the PKA transition state and phosphoryl transfer mechanism suggest that Mg2 yields greater stabilization of the transition state than Mg1 and may thus be more important for catalysis.[20−22] Therefore, there is some uncertainty about the roles of the two magnesium ions.

Adding further importance to understanding the roles of the magnesium ions is the fact that ATP exists as a complex with magnesium in physiological settings, and in many crystal structures only one metal ion is present. Often, however, the γ-phosphate in these structures does not seem to be ideally oriented for phosphoryl transfer.[23,24] In PKA and some other kinases, two metal ions are bound. More recently a comprehensive analysis of cyclin dependent kinase 2 (CDK2) showed that two metal ions are required for the phosphoryl transfer reaction.[25,26] CASK is a highly unusual kinase, the only one known so far, that requires no magnesium ions.[27] Some kinases, such as PKA and CDK2, are inhibited by increases in magnesium concentration while others show no effect or increased activity in the presence of excess magnesium.[14,25,26,28] Therefore, magnesium ions can display complex regulatory roles on protein kinase function. A more detailed understanding of the different roles for magnesium ions in different protein kinases may provide a better understanding of kinase function which could aid in our understanding of activating mutations involved in disease or improve the design of inhibitors of kinases for therapeutic purposes.

In addition to the magnesium ions, there are several conserved residues that are important for phosphoryl transfer. Asp166, which is completely conserved in kinases and may act as a catalytic base, is thought to position the substrate for phosphoryl transfer, and mutation of this residue causes severe defects in phosphoryl transfer.[29,30] Additionally, Lys72 in β-strand 3 forms a salt bridge with Glu91 from the C-helix, and Lys72 helps position ATP for phosphoryl transfer by binding to the α- and β-phosphates of ATP. This lysine residue is essential for catalysis, and it is often mutated in kinases to make "kinase dead" mutants even though this mutation does not abolish ATP binding.[29,31−33] Furthermore, Lys168 forms a hydrogen bond with the γ-phosphate of ATP and may stabilize the transition state or possibly aid in the phosphoryl transfer reaction.[21,34]

To better understand substrate binding and catalysis by PKA, the catalytic subunit was crystallized with a substrate peptide SP20 corresponding to the 20 amino acid inhibitor peptide derived from the endogenous protein inhibitor PKI (5−24) with two mutations that convert it from an inhibitor to a substrate (N20A, A21S).[35,36] In addition to SP20, the protein was crystallized with adenosine-5′-(β,γ-imido)triphosphate (AMP-PNP), which is a generally nonhydrolyzable analog of ATP where the atom bridging the β- and γ-phosphates is replaced with a nitrogen.[37] To our surprise, despite using AMP-PNP, protein crystals grown under certain conditions displayed clear phosphoryl transfer of the γ-phosphate of AMP-PNP onto the P-site serine. Although AMP-PNP is generally used as a nonhydrolyzable analog of ATP, there are some reports of AMP-PNP being hydrolyzed and serving as a substitute for ATP although no kinases are reported to utilize AMP-PNP to our knowledge.[37−40]

We obtained two crystal structures of the C-subunit where both products are trapped in the crystal lattice. One structure refined to 1.55 Å resolution of a crystal analyzed approximately 3 months after appearance displays two states of the protein. 55% of the protein is modeled with intact AMP-PNP and an unphosphorylated substrate, and 45% is modeled with the products of phosphoryl transfer which are AMP-PN and a phosphorylated substrate. Another structure of a crystal harvested approximately 5 months after appearance was refined to 2.15 Å resolution and displays complete phosphoryl transfer. These structures offer unprecedented insights into the midpoint and end point of kinase phosphoryl transfer allowing for a characterization of the roles of the magnesium ions and yielding information about the steps and mechanisms involved in the reaction turnover. We conclude that, contrary to some previous reports, Mg2 likely binds within the active site first followed by Mg1 and binding of both ions not only is necessary for optimum phosphoryl transfer but also slows product release following transfer. Following transfer, Mg1 leaves the active site which then allows for Mg2-ADP release. Release of Mg1 is likely an important aspect of product release and likely explains why ADP release is rate-limiting at high magnesium concentrations due to the continued occupancy of both magnesium binding sites following phosphoryl transfer.

EXPERIMENTAL METHODS

Purification of the C-Subunit Proteins. The nonmyristylated WT protein was expressed and purified as described previously.[41] The myristylated C-subunit protein was prepared by coexpression with yeast NMT as described previously[42] and purified using a protocol described previously.[43] The myristylated C-subunit utilized for crystallography was a mixture of doubly and triply phosphorylated protein with all protein phosphorylated on Thr197 and Ser338 and about 50% phosphorylated on Ser139. The nonmyristylated C-subunit utilized for crystallization was triply phosphorylated on Ser10, Thr197, and Ser338.

Crystallization. The AMP-PNP, Mg^{2+}, and SP20 complexes were crystallized under similar conditions utilized for previous C-subunit structures.[43−45] The C-subunit protein was dialyzed overnight into 50 mM bicine, 150 mM ammonium acetate, and 10 mM DTT at pH 8.0. This protein was concentrated to 8−10 mg/mL. Immediately preceding crystallization, the protein was combined in an approximately 1:10:20:5 molar ratio of protein:AMP-PNP:Mg^{2+}:SP20 with the AMP-PNP dissolved in 0.1 M Tris pH 7.0 and the Mg^{2+} and SP20 dissolved in water. The protein was crystallized using hanging drop vapor diffusion with 2−6% 2-methyl-2,4-pentanediol (MPD) dissolved in DI water as the well solution. An important note is that phosphoryl transfer of AMP-PNP was only seen when low percentages of MPD were used in the well solution (6% MPD or less) and transfer was not seen with higher MPD percentages.[43] The protein was crystallized using 8 μL drops of 1:1 protein to well solution, and 80−150 μL of methanol were added to the 1 mL well solution immediately before sealing the well. These crystals were grown at 4 °C. Both crystal structures presented here were obtained from drops with the well solution containing 2% MPD. 80 μL of methanol were added to the well for the 1.55 Å structure, and 125 μL of methanol were added to the well for the 2.15 Å structure.

Although it is unclear why low MPD concentrations seem to be required for significant phosphoryl transfer in the crystals, the crystallization conditions may be a contributing factor. High MPD concentrations increase the viscosity of the solution which may inhibit the movement and possible conformations that can be adopted by the protein, and this may have prevented phosphoryl transfer in our earlier structures.[43] Another possibility is that MPD, a nonpolar compound, will decrease the polarity of the crystal solution. By decreasing the polarity of the solution, MPD may effectively inhibit phosphoryl transfer by neutralizing the magnesium ions or protein residues which are critical for phosphoryl transfer. Additionally, the decreased polarity would also inhibit phosphoryl transfer because polar solvents would be preferred to stabilize the transition state and provide solvent molecules to aid in the reaction.

Data Collection and Refinement. The crystals were flash cooled in liquid nitrogen with cryoprotectant solution (12% MPD and 15% glycerol). The 1.55 Å data set was collected on a crystal harvested approximately 3 months after initial appearance, and the 2.15 Å data set was from a crystal harvested approximately 5 months after initial appearance. The crystal structures were each obtained from one crystal: however, the 2.15 Å structure is from two separate data sets of the same crystal that were merged. Because one data set used a longer exposure time, it allowed refinement to a slightly higher resolution than the first set. The two sets were merged to increase the completeness of the data set. Data were collected on the synchrotron beamline 8.2.1 for the 1.55 Å structure and on beamline 8.2.2 for the 2.15 Å structure of the Advanced Light Source, Lawrence Berkeley National Laboratories (Berkeley, California). For each crystal structure, the data were integrated using iMOSFLM.[46] Both complexes crystallized in the $P2_12_12_1$ space group similar to previous structures. Molecular replacement was carried out using Phaser[47] with 3FJQ[48] as a search model. The refinement was performed using refmac5,[49] and model building was done in Coot.[50] Clear density was visible for phosphoryl transfer in both structures. The 1.55 Å structure showed electron density representing two states of the protein which were with and without phosphoryl transfer. The structure was refined using different percentages of reactant and product states, and 45% phosphoryl transfer yielded the best fit to the electron density. The 2.15 Å structure only showed density for phosphoryl transfer with no density for the intact γ-phosphate of AMP-PNP. However, there was some negative density at the P-site phosphate with full transfer modeled, and therefore, the structure was modeled with 70% phosphoryl transfer. The negative density may arise from some AMP-PNP that hydrolyzed prior to crystallization or that hydrolyzed without phosphoryl transfer. Another note about the refinement is that the Gly-rich loop in the 1.55 Å structure shows some positive electron density that may represent the presence of some molecules that adopt a lower conformation of the loop. Multiple conformations may be adopted due to the presence of both phosphoryl transfer and no transfer, but the majority of the protein is in the conformation modeled. The structures were refined to R_{work}/R_{free} of 17.2%/19.4% and 18.7%/22.8% for the 1.55 Å (4HPU) and 2.15 Å (4HPT) structures respectively. Data collection and refinement statistics are shown in Supplemental Table 1.

Mass Spectrometry Analysis of Protein Crystals. Preceding mass spectrometry analysis, the protein crystals were washed by sequentially transferring the crystals through 5 drops of fresh well solution (2% MPD) to remove any protein/peptide arising from the solution rather than the crystal. The sample was loaded to a C18 precolumn (360 μm O.D. × 100 μm I.D., 5 μm Zorbax SB-C18, 10 cm packing). The precolumn was connected via Teflon tubing to a C18 analytical column (360 μm O.D. × 75 μm I.D., 5 μm Zorbax SB-C18, 10 cm packing) with an integrated emitter tip (2−4 μm I.D.). Peptides were eluted into an LTQ Orbitrap mass spectrometer (ThermoFisher Scientific, San Jose, CA) with an Agilent 1100 HPLC system. A precolumn splitter was used so that the flow rate out of the emitter tip was about 100 nL/min throughout the gradient. The HPLC gradient was 0−40% B in 30 min (Buffer A: 0.1% formic acid; Buffer B: 90% ACN in 0.1% formic acid). The mass spectrometer was operated in a targeted mode where m/z ratios of +2, +3, and +4 of both the phosphorylated and nonphosphorylated peptide were targeted throughout the entire HPLC gradient. The isolation window for precursor masses were set to 0.5 Da. The dynamic exclusion option was selected with a repeat count of 1, a repeat duration of 0.5 min, and an exclusion duration of 1 min. For data analysis, the m/z ratios for +2, +3, and +4 of the phosphorylated and nonphosphorylated peptides were extracted.

Generating $F_o - F_c$ Omit Maps. The maps displayed in Figures 2 and 3C were generated by omitting different elements from the final model of the structures. The structures were then refined with the components omitted using 10 or more cycles of restrained refinement, and $F_o - F_c$ maps were generated using the FFT program in the CCP4 suite.[49]

Measurement of Phosphoryl Transfer of AMP-PNP to RIIβ *in vitro*. The purified C-subunit of PKA was incubated with purified RIIβ; purification of RIIβ is described elsewhere,[51] alone and with ATP or AMP-PNP in 0.1 M MOPS, 10 mM $MgCl_2$ at pH 7.0. The concentration of ATP and AMP-PNP used in the reaction buffer was 1 mM when the nucleotides were included. The reaction mixture contained approximately 300 nM C-subunit and 300 nM RIIβ. The reaction was incubated at room temperature for the first 30 min and was then kept at 4 °C. Time points of the reaction were quenched at 30 min, 1 day, and 2 days by taking samples of the reaction mixture, mixing 1:1 with SDS−PAGE sample buffer, and heating the samples for 10 min at 70 °C. These samples were analyzed by Western blot with antibodies against the C-subunit (BD Biosciences), RIIβ (Biomol), and against R-R-X-phosphorylated S/T, the PKA consensus sequence which RIIβ contains at its inhibitor site[51] (Cell Signaling Technology). The level of phosphorylation with AMP-PNP was quantified using ImageJ with the amount of phosphorylated RIIβ for each time point with ATP treated as 100% phosphorylation and with the values normalized to the total amount of RIIβ.

RESULTS

1.55 Å Structure Displaying Partial Phosphoryl Transfer of the γ-Phosphate of AMP-PNP. The myristylated C-

dx.doi.org/10.1021/ja312237q | J. Am. Chem. Soc. 2013, 135, 4788−4798

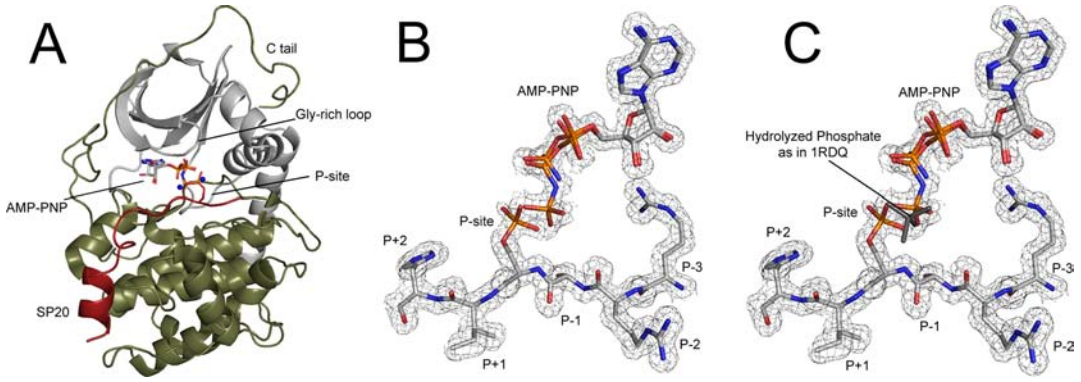

Figure 1. Crystal structure of PKA displays partial phosphoryl transfer of AMP-PNP onto a substrate peptide. (A) The overall 1.55 Å PKA structure, 4HPU, is displayed in cartoon representation with the small lobe (12−126) colored white, large lobe (127−350) colored olive, SP20 colored red, P-site serine and ANP-PNP shown in stick representation and colored by element, and magnesium ions shown as spheres and colored blue. (B) The $2F_o - F_c$ electron density map contoured to 1 σ is displayed showing partial phosphoryl transfer and partial intact AMP-PNP. The structure is modeled with 45% phosphoryl transfer, 55% reactants. (C) The same density as in B with the free phosphate from 1RDQ[45] displayed in gray to illustrate that the electron density corresponds to phosphoryl transfer and not hydrolyzed, free phosphate.

subunit was crystallized with AMP-PNP, magnesium, and SP20, and the structure was refined to 1.55 Å resolution (Figure 1A). Despite using AMP-PNP, the structure shows clear phosphoryl transfer of the γ-phosphate of AMP-PNP onto the substrate serine residue. There is density both for the γ-phosphate on AMP-PNP and for phosphorylated serine on SP20 (Figure 1B). Therefore, these crystals contain some protein that has undergone phosphoryl transfer and some that remains in the reactant state with intact AMP-PNP and the unphosphorylated substrate. The structure was refined with different percentages of phosphoryl transfer, and 45% phosphoryl transfer, 55% reactant state yielded the best fit to the electron density.

One previously reported crystal structure, 1RDQ, showed partial hydrolysis of ATP, but since 1RDQ was crystallized with IP20 which contains Ala at the P-site, the phosphate remained as free phosphate within the structure.[45] To verify that the structure reported here corresponds to phosphoryl transfer and not hydrolysis, we aligned the free phosphate from 1RDQ with this structure. This alignment clearly shows that the hydrolyzed phosphate, as observed in 1RDQ, does not fit the electron density in this structure (Figure 1C). To further verify phosphoryl transfer, the structure was modeled and refined with AMP-PNP and no phosphoryl transfer. The resulting $F_o - F_c$ map shows positive electron density on the P-site serine (Figure 2A). Alternatively, if the structure is refined with ADP and phosphorylated SP20, the $F_o - F_c$ map shows positive electron density for the γ-phosphate of AMP-PNP (Figure 2B). Finally, if the structure is modeled without phosphoryl transfer and with ADP, the $F_o - F_c$ map shows positive electron density for both phosphoryl transfer and the γ-phosphate of AMP-PNP (Figure 2C). To further confirm the presence of phosphoryl transfer and to ensure that the transfer was present in the crystal and not a result of radiation damage on the X-ray beam, protein crystals were harvested, washed thoroughly, and analyzed by mass spectrometry. Mass spectrometry confirmed the presence of both phosphorylated and unphosphorylated SP20 within the crystal (Supplemental Figure 1, Supplemental Table 2) verifying the results from the crystal structure.

To further verify that AMP-PNP can be utilized for phosphoryl transfer by the C-subunit, the C-subunit was incubated with AMP-PNP and RIIβ *in vitro*. RIIβ contains a C-subunit phosphorylation site at its inhibitor site.[51] Phosphorylation of RIIβ with AMP-PNP was monitored by Western blot analysis using an antibody against the phosphorylated PKA substrate. AMP-PNP promoted the phosphorylation of RIIβ in a time-dependent manner, albeit very slowly (Supplemental Figure 2). However, the transfer appears to occur much more quickly with RIIβ in solution than it did with SP20 in the crystallization conditions yielding about 80% transfer compared to ATP after 2 days. The different rates may be due to the different conditions used for crystallization such as different pH values, pH 8.0 during crystallization versus pH 7.0 in solution, and the presence of MPD and methanol during crystallization, which are all likely to affect the transfer rate. It is also possible that RIIβ is phosphorylated with AMP-PNP more readily than SP20. Additionally, turnover may proceed more slowly in a crystalline state, once the protein crystallizes, than in solution due to conformational constriction. However, both the crystal structure and solution studies show that the C-subunit can utilize AMP-PNP for phosphoryl transfer but at a much slower rate than with ATP.

2.15 Å Structure Displays Complete Phosphoryl Transfer of AMP-PNP. The 1.55 Å crystal structure was of the myristylated WT protein and shows strong density for 10 of the 14 carbon atoms of myristic acid (Supplemental Figure 3). To test whether phosphoryl transfer was a result of myristylation and whether phosphoryl transfer increases over time in the crystal as it does in solution (Supplemental Figure 2), the nonmyristylated WT protein was crystallized and data were collected on a crystal approximately 5 months after initial appearance compared to 3 months after crystal appearance for the 1.55 Å structure. This structure was refined to 2.15 Å resolution and displays complete phosphoryl transfer.

The electron density map of the phosphorylation site shows density for phosphoryl transfer with no density for an intact γ-phosphate on AMP-PNP (Figure 3A). Also, again, the density corresponds to phosphoryl transfer and not hydrolysis as seen in 1RDQ[45] (Figure 3B). To further confirm complete phosphoryl transfer, the crystal structure was refined using a model without P-site serine phosphorylation and with ADP modeled in the active site. The resulting $F_o - F_c$ electron density map from this structure is shown in Figure 3C. This map only shows positive electron density for phosphoryl transfer with no density for the γ-phosphate of AMP-PNP confirming complete phosphoryl transfer. An important note is that the 2.15 Å structure is modeled with 70% phosphoryl

dx.doi.org/10.1021/ja312237q | J. Am. Chem. Soc. 2013, 135, 4788−4798

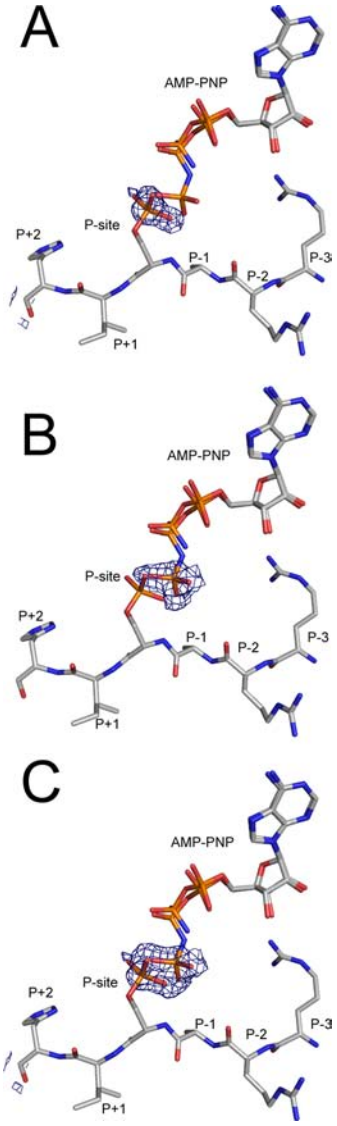

Figure 2. Partial phosphoryl transfer is further verified with $F_o - F_c$ maps with different components omitted. The $F_o - F_c$ electron density maps contoured to 3σ are shown when AMP-PNP and no phosphoryl transfer are modeled (A); when complete phosphoryl transfer to the P-site serine and ADP are modeled (B); and when no phosphoryl transfer and ADP are modeled (C). When either P-site phosphorylation (A) or the γ-phosphate of AMP-PNP (B) are excluded from the model, the electron density map clearly shows positive electron density that corresponds to each phosphate group. This finding is also confirmed when both P-site Ser phosphorylation and the γ-phosphate of AMP-PNP are excluded from the model (C).

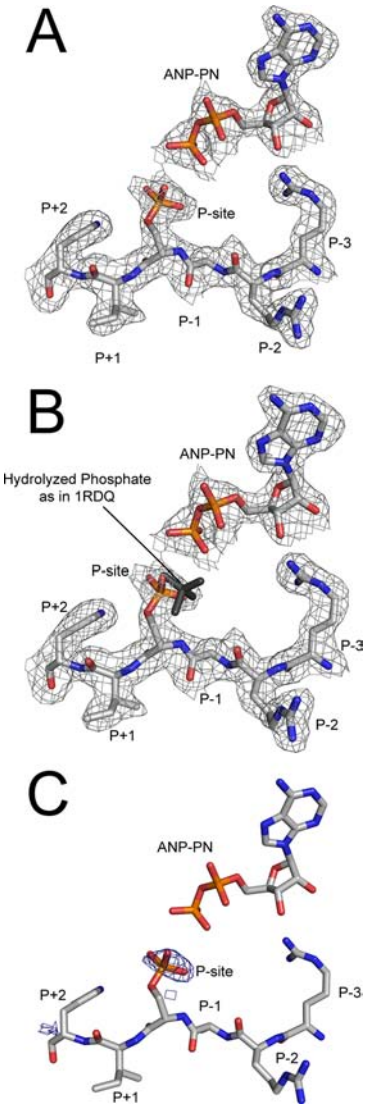

Figure 3. The 2.15 Å crystal structure displays complete phosphoryl transfer of AMP-PNP onto the substrate peptide. (A) The $2F_o - F_c$ electron density map at 1σ is displayed for 4HPT showing electron density for complete phosphoryl transfer. (B) The hydrolyzed phosphate from 1RDQ[45] is aligned with this structure and colored gray showing that the electron density corresponds to phosphoryl transfer and not hydrolyzed phosphate. (C) The $F_o - F_c$ electron density map generated from a model with ADP and no phosphoryl transfer modeled in the structure is displayed at 3σ showing positive electron density for phosphoryl transfer with no density for the γ-phosphate of AMP-PNP.

transfer because, despite the lack of density for the γ-phosphate of AMP-PNP, there was some negative density at the phosphoryl transfer site with full transfer modeled, which may arise from AMP-PNP that hydrolyzed prior to crystallization or hydrolyzed without transfer.

Changes in the Magnesium Ions with Partial versus Complete Phosphoryl Transfer. Alignment of the two structures shows mostly overlap between the P-site residues within each structure. However, one interesting difference between the two structures involves the magnesium ions. In the 2.15 Å structure, which has undergone complete phosphoryl transfer, Mg1 is partially, if not completely, absent from the active site. Mg1 is modeled into the structure, but there is much less electron density for Mg1 than typically seen for magnesium ions and much less density compared to the 1.55 Å structure (Figure 4A, B). Correspondingly, Mg1 also has much higher B-factors than typically seen for magnesium or manganese ions in PKA structures (Supplemental Table 3), and the increased B-factor values are only seen for Mg1 and not Mg2, which indicates that it is not partial loss of both ions but only Mg1. Additionally, Mg1 is moved away from Asp184 compared to most structures (Supplemental Table 3, Figure 5A, B), which is not typical for Mg1 and occurs without equivalent changes in Mg2. These findings suggest that Mg1 was partially expelled from the active site following phosphoryl transfer or may have been completely expelled and replaced by a water molecule.

dx.doi.org/10.1021/ja312237q | J. Am. Chem. Soc. 2013, 135, 4788−4798

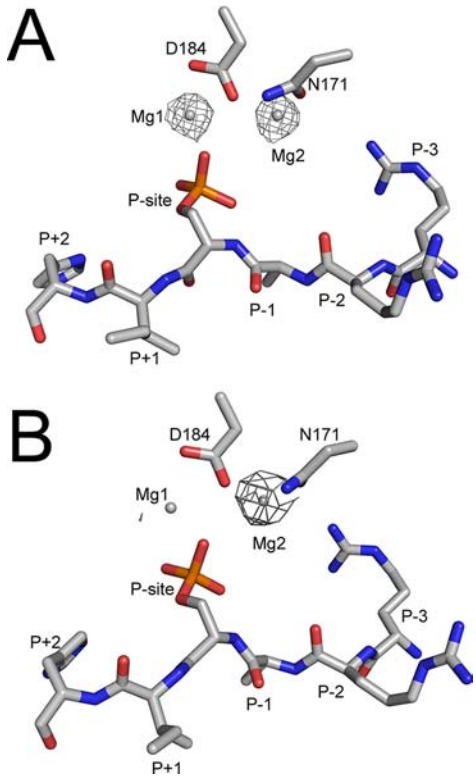

Figure 4. Mg1 is expelled from the active site following complete phosphoryl transfer. The $2F_o - F_c$ electron density map at 2σ is displayed for the magnesium ions in the 1.55 Å, partial phosphoryl transfer structure, 4HPU (A), and in the 2.15 Å, complete phosphoryl transfer structure, 4HPT (B). There is much less electron density for Mg1 than typically seen for magnesium ions in the 2.15 Å complete phosphoryl transfer structure which indicates partial, if not complete, loss of this magnesium ion.

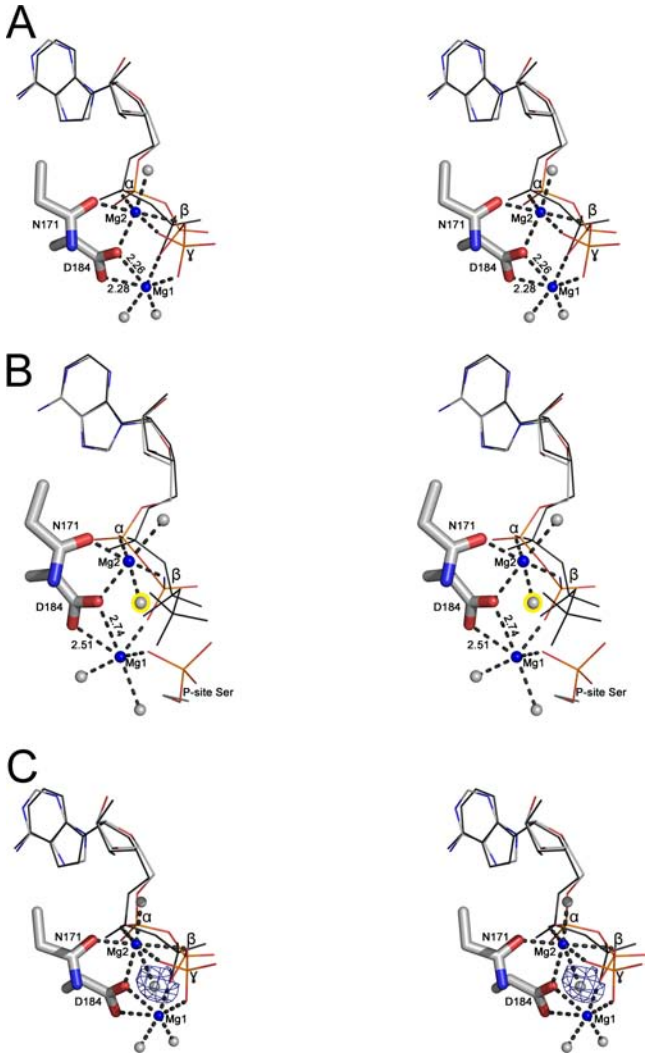

Figure 5. Coordination of the magnesium ions before and after phosphoryl transfer. (A) A stereoview of the magnesium ions in the 1.55 Å partial phosphoryl transfer structure is displayed. AMP-PNP is colored by element, AMP-PN (without γ-phosphate) is colored black, water molecules are colored gray, and magnesium ions are colored blue. The distances between Asp184 and Mg1 are shown in angstroms. (B) A stereoview of the magnesium ions in the 2.15 Å complete phosphoryl transfer structure is shown. The AMP-PN from the structure is colored by element, water molecules are colored gray, magnesium ions are colored blue, and AMP-PNP from the 1.55 Å partial phosphoryl transfer structure is aligned and shown in black. Mg2 recruits an additional water molecule that fulfills the vacancy left after transfer of the γ-phosphate highlighted in yellow. (C) Coloring is the same as in panel A. The $F_o - F_c$ electron density map at 3σ is shown in blue for the area near the new water molecule recruited by Mg2 following phosphoryl transfer in the 1.55 Å partial phosphoryl transfer structure. Thus Mg2 immediately recruits this new water molecule which was included in the final model.

The structure was modeled with a magnesium ion because it is potentially coordinated with six elements, as would be expected for a magnesium ion, but likely represents either partial occupancy of this site with Mg1 or may result from complete loss of this ion and replacement with a water molecule.

Another interesting aspect of these structures is the coordination of the magnesium ions. In the 2.15 Å structure, Mg2 recruits a new water molecule to maintain an octahedral geometry following transfer of the γ-phosphate (Figure 5A, B). Also, this recruited water molecule is present in the 1.55 Å crystal structure that shows partial phosphoryl transfer. Initially there was positive electron density in the 1.55 Å structure near the γ-phosphate that could not be explained, but the 2.15 Å structure helped identify this density as corresponding to this water molecule that is recruited following phosphoryl transfer to maintain an octahedral coordination geometry of Mg2 (Figure 5C). Therefore, these results exemplify the strong binding character of Mg2, which supports its role in phosphoryl transfer, as it immediately binds an additional water molecule following phosphoryl transfer. In contrast, Mg1 is partially, if not completely, removed from the active site following phosphoryl transfer despite the fact that this ion should presumably be able to bind since all elements are present for it to maintain similar binding as in the intact AMP-PNP state (Figure 5A, C). Despite transfer of the γ-phosphate, Mg1 should still be able to coordinate with the transferred phosphate and all five other Mg1 binding elements still remain. Also, previous biochemical studies suggested that Mg1 and Mg2 bind with equal affinity with ADP.[10]

DISCUSSION

By using a substrate version of IP20, which has a much slower off-rate than other peptide substrates, we were able to capture the phosphoryl transfer step in the crystal lattice. The slow off-rate of SP20 may have facilitated the transfer, even with AMP-PNP, and the retention of both products. The substrate

dx.doi.org/10.1021/ja312237q | J. Am. Chem. Soc. 2013, 135, 4788−4798

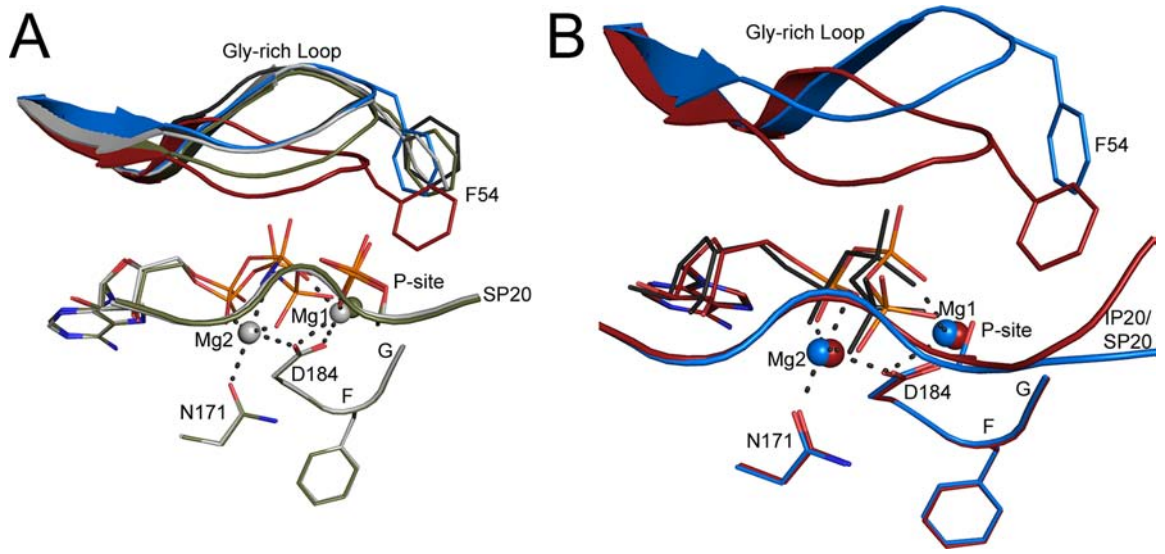

Figure 6. Changes in the Gly-rich loop with substrates bound and following phosphoryl transfer. (A) The Gly-rich loop is slightly raised in the structures reported here, full transfer (4HPT) depicted in olive and partial transfer (4HPU) depicted in gray, compared to the fully closed structure typically observed with ATP and IP20 (depicted in red from PDB: 3FJQ[48]). The raised loop may result from the presence of a serine rather than alanine residue at the P-site as evident from previous C-subunit structures containing a substrate bound at the active site such as SP20 (depicted in blue from PDB: 4DG0[43]) and RIIβ(108−268) (depicted in black from PDB: 3IDB[52]). (B) 4DG0 and 3FJQ are depicted in the same colors as panel A with ATP from 3FJQ colored by element and AMP-PNP from 4DG0 colored black. This alignment highlights that the raised Gly-rich loop may be the result of substrate binding alone and not phosphoryl transfer since 4DG0 which was bound to SP20 but exhibited no phosphoryl transfer also has a raised Gly-rich loop.

complex with SP20 solved earlier showed how the Gly-rich loop is perturbed in a minimal way when the P-site Ala is replaced by Ser,[43] and a similar shift was observed in the Gly-rich loop with the RIIβ subunit bound,[52] which is also a substrate (Figure 6A−B). The glycine-rich loop clearly senses what is present at the P-site. The loop changes a bit more following complete transfer of the phosphate to SP20, but the changes are minimal. The fact that neither the backbone geometry nor the temperature factors for the peptide change significantly when SP20 is phosphorylated suggests that both products are trapped. This may be unique to the SP20 structure, which binds with such high affinity and docks to an important hydrophobic groove near the active site. Despite extensive structural, computational, and biochemical studies of PKA, there is still uncertainty and debate about the mechanistic details of catalysis and, in particular, about the roles of the essential magnesium ions in phosphoryl transfer and the steps involved in the rate-limiting step of ADP release. The structures described here allowed us to characterize the reaction progression by PKA. By trapping both products in the crystal lattice we have an opportunity to dissect these critical events in the catalytic process. We obtained one of the highest resolution WT PKA structures to date, which displays 45% phosphoryl transfer. Without these conditions that yield slow phosphoryl transfer of AMP-PNP, it would be difficult to obtain a structure displaying partial phosphoryl transfer. This phosphoryl transfer midpoint structure and the end point 2.15 Å crystal structure displaying complete phosphoryl transfer allowed us to explore in new ways the PKA phosphoryl transfer reaction steps and the roles of the two magnesium ions.

We find that Mg2 recruits a water molecule immediately following phosphoryl transfer to maintain an octahedral coordination state. This recruited water molecule is present in both the partial phosphoryl transfer and complete phosphoryl transfer structures due most likely to the strong binding character of Mg2, which may help to catalyze the phosphoryl transfer reaction and/or stabilize the transition state. Additionally, we find that Mg1 is partially, if not completely, expelled following phosphoryl transfer, which implies that it may not bind as strongly and possibly may not influence the active site as much as Mg2. There is no obvious reason why Mg1 should be expelled following phosphoryl transfer since six binding partners of Mg1 are still present. Also, this finding contradicts previous reports that suggested that Mg1 and Mg2 bind with equal affinity with ADP.[10] The concentration of magnesium in the crystal drop is approximately 2.5 mM. This is a relatively high concentration that is much higher than typical physiological concentrations[17,19] and would, presumably, allow for occupation of the Mg1 site if favorable. Therefore, this structure suggests that Mg1 may not bind as tightly as Mg2 following phosphoryl transfer. Indeed, the inhibitory effects of high magnesium concentrations may arise from occupation of both magnesium sites even after phosphoryl transfer, which may slow down the rate-limiting step of ADP release. This mode of magnesium inhibition was proposed previously[14] and seems consistent with the implications of these crystal structures. The single caveat which may promote the release of Mg1 is that we used AMP-PNP instead of ATP, and the nitrogen atom could facilitate the release of Mg1.

Mg1 leaving the active site following phosphoryl transfer may help to answer the important question of how ADP release, the rate-limiting step at high magnesium concentration, is achieved. Computational studies performed to analyze how ADP is released from PKA when two magnesium ions are bound suggested that release was so energetically unfavorable that it would require local unfolding at the active site or large global conformation changes in the protein for release.[53] Consequently, the authors argue that one or both magnesium ions may need to be expelled prior to ADP release. Based on

dx.doi.org/10.1021/ja312237q | J. Am. Chem. Soc. 2013, 135, 4788−4798

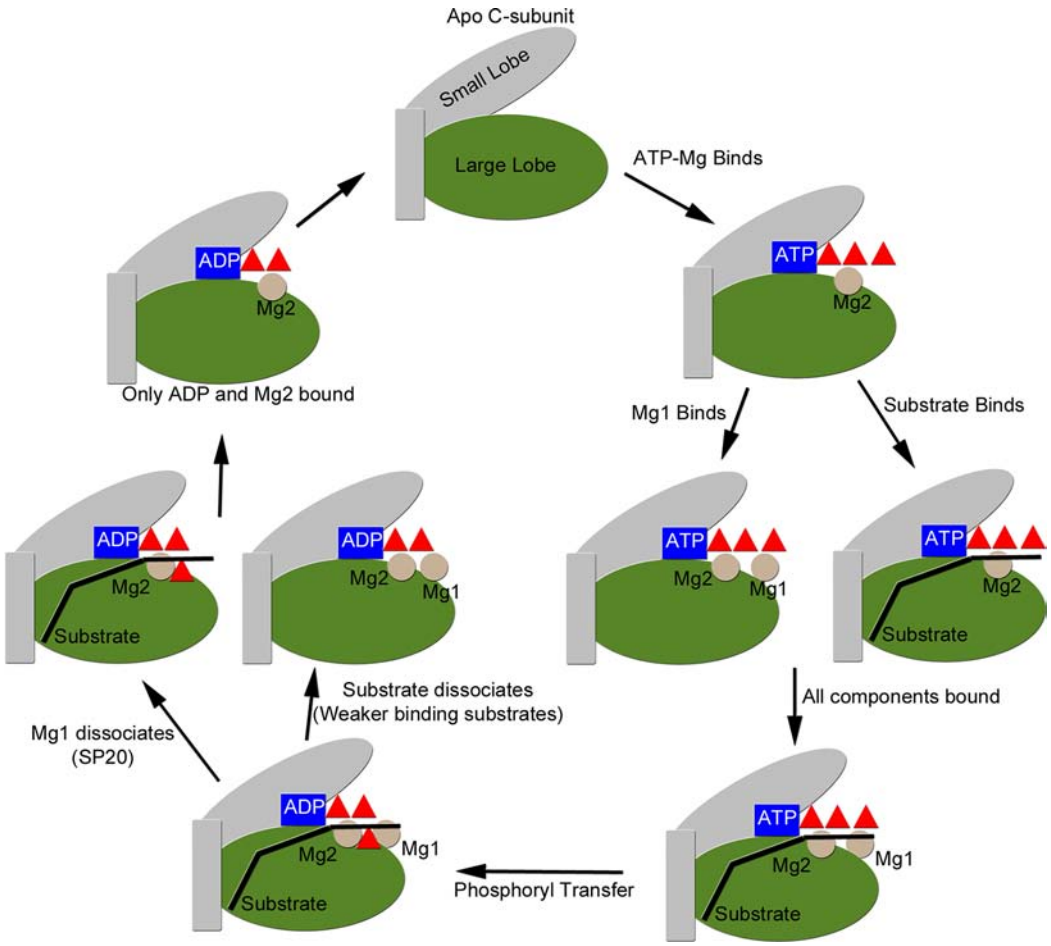

Figure 7. Catalytic cycle of PKA. A similar cycle is also predicted for CDK2.[26]

the results described here, we propose that Mg1 is the ion that leaves following phosphoryl transfer and this would allow for ADP release.

The structures described here as well as previous crystal structures begin to elucidate the important aspects and steps involved in phosphoryl transfer (Figure 7). An important recent result is the crystal structure of PKA obtained under low magnesium concentration, which shows electron density for only Mg2.[19] This structure suggests that Mg2 may bind within the active site first with ATP. It is possible that recognition of the Mg-ATP complex may involve shuttling between the negatively charged residues at the active site including Asp184 and Asp166. Based on the Kovalevsky structure, however, it appears that when Mg-ATP is docked stably into the active site cleft it binds preferentially to the Mg2 site between Asn171 and Asp184. The structures presented here suggest, furthermore, that Mg2 remains in the active site following phosphoryl transfer while Mg1 is expelled, at least in the presence of AMP-PNP. In addition, Mg2 recruits an additional water molecule following phosphoryl transfer to retain an octahedral coordination geometry (Figure 5B). Taken together, these findings suggest that Mg2 may bind first and exhibits strong binding character. Mg1 helps to position the γ-phosphate of ATP for transfer but is expelled from the active site following phosphoryl transfer to allow for ADP release. ADP and Mg2 are likely to be the last entities remaining in the active site that are most likely released together or may remain until being replaced by another ATP and magnesium ion (Figure 7). We cannot comment on the order of the addition of substrates but assume that in the cell with physiological substrates ATP-Mg2 will bind first and then either the peptide or Mg1. With the high affinity phosphorylated SP20 peptide and ADP, it is the Mg1 that is released first. Whether the phosphorylated substrate or the ADP-Mg2 is released next or whether they leave simultaneously is unknown. With physiological substrates, it is likely the phosphorylated protein that will leave first.

This mechanism of phosphoryl transfer progression and turnover may be a general pathway utilized by many, if not all, protein kinases. Given the highly conserved nature of the active site residues of protein kinases, in particular Asp184 of the "DFG" motif and Asp166 the "catalytic base," we predict that all kinases will likely utilize two metal ions, but the details of catalysis and product release may be regulated differently in different kinases. The DFG motif, for example, is highly regulated in many kinases, and it is serving as the "keeper" of Mg1 both positioning it for transfer and also facilitating its release. Recent crystal structures of cyclin dependent kinase 2 (CDK2) suggest a similar process of substrate turnover for this kinase.[26] Many previous CDK2 crystal structures bound to ATP or ATP-analogues displayed one magnesium ion within the active site, analogous to Mg2 in PKA structures, suggesting initially that CDK2 may utilize a single metal ion for phosphoryl transfer. However, a crystal structure of a transition state mimic of CDK2 identified two magnesium ions in the active site which are analogous to Mg2 and Mg1 from PKA, and biochemical experiments suggested that the enzyme utilizes two

dx.doi.org/10.1021/ja312237q | J. Am. Chem. Soc. 2013, 135, 4788−4798

magnesium ions during turnover.[25] Furthermore, recent structures of CDK2 bound to ADP showed the presence of one or two magnesium ions (Mg2 or Mg1 and Mg2) bound with ADP.[26] Therefore, these studies independently identified a similar mode of phosphoryl transfer progression in CDK2. The authors also argue that CDK2 binds Mg2 first, but Mg1 must also bind for optimal turnover. After phosphoryl transfer, having two magnesium ions bound to ADP slows product release resulting in a decrease in turnover rate at high magnesium concentration in CDK2 as is also seen in PKA. Based on the two structures of CDK2 bound to ADP, it appears that Mg1 binds less tightly following phosphoryl transfer which then allows for ADP release. Therefore, the findings from our PKA phosphoryl transfer structures may present a general mechanism utilized by many, if not all, protein kinases. Additionally, the structures described here trapped the enzyme at different steps during phosphoryl transfer and trapped both products. The results from these structures are thus likely to represent steps in the reaction progression and are not affected by crystallization soaking conditions that may have yielded the magnesium differences in the CDK2 structures.

The catalytic mechanism of protein kinases, like the roles of the magnesium ions, remains unresolved. There are two mechanisms proposed for phosphoryl transfer by protein kinases which are an associative mechanism and a dissociation mechanism.[20,21,25,30,34] The main differences between these mechanisms are the transition states and which group accepts the hydrogen atom from the substrate residue. The associative mechanism forms a trigonal bipyramidal transition state with a −3 charge where bond formation with the substrate serine begins before the bond between the β- and γ-phosphate is completely broken, and the proton on the substrate residue is accepted by the incoming γ-phosphate. The dissociative mechanism involves a complete break in the leaving group yielding a metaphosphate with −1 charge, and the conserved aspartate residue, Asp166 in PKA, acts as a catalytic base that accepts the proton from the substrate residue. There has been some debate about the mode of phosphoryl transfer, but the majority of recent studies suggest a dissociative mechanism.[20,21,30]

The crystal structures reported here depict the starting point and end point of the phosphoryl transfer reaction and do not represent a transition state, which makes it difficult to make conclusions about the mechanism of phosphoryl transfer. However, there is a PKA transition state mimic structure[34] and CDK2 transition state mimic structure,[25] and when comparing the structures reported here with the transition state structures, some insights may be gleaned about the mechanism of phosphoryl transfer. First of all, the residues at the active site in these phosphoryl transfer structures are very similar to the transition state PKA structure except for the raised Gly-rich loop in these structures (Figure 6). However, there are a couple of interesting differences between these structures and the transition state mimic. The biggest difference between these structures and the transition state mimic, 1L3R,[34] is the orientation of the substrate serine, Ser21 in the peptide, and the position of Asp166, the putative catalytic base (Supplemental Figure 4A, B). In the transition state mimic structure, the substrate serine is facing Asp166 forming a hydrogen bond with this residue, and in this state, the serine residue is primed for an in-line transfer of the phosphate. By contrast, in these phosphoryl transfer structures the serine residue is flipped away from Asp166 (Supplemental Figure 4A, B).

It could be argued that this flip occurs following phosphoryl transfer as a means to initiate substrate release by, for instance, forcing the Gly-rich loop to rise because this conformation would clash with Phe54 in the fully closed state (Supplemental Figure 4A, B). However, several previous kinase structures bound to the substrate and AMP-PNP showed that the substrate serine residue is flipped away from Asp166 before phosphoryl transfer occurs. In previous structures of the C-subunit bound to SP20 and AMP-PNP without phosphoryl transfer, Ser21 is pointed away from Asp166[43] (Supplemental Figure 4C). Additionally, a structure of the C-subunit bound to AMP-PNP and a truncated form of RIIβ, which is a substrate for the C-subunit, also showed the P-site serine facing away from Asp166[52] (Supplemental Figure 4C). Finally, a structure of Akt/PKB bound to a substrate and AMP-PNP also adopted this conformation with the serine residue facing away from the aspartate residue[54] (Supplemental Figure 4C). Therefore, this conformation of the substrate residue may precede phosphoryl transfer. However, in the CDK2[25] and PKA[34] transition state mimic structures, the substrate residue is facing the putative catalytic base aspartate residue (Supplemental Figure 4D).

The positioning of the serine residue away from Asp166 would seem to contradict the favored dissociative mechanism because the residue is not facing the catalytic base. However, computational studies addressing the mechanism of phosphoryl transfer suggested that the potential hydrogen bond between Asp166 and the substrate residue is actually quite weak in the reactant state and becomes very strong only during the transition state.[20] It is not until late in the reaction that Asp166 accepts the proton from the substrate residue. Therefore, these structures may support this mode of reaction progression. It appears that Asp166 does not yield a strong effect on the substrate residue in the reactant state, which may be why the substrate serine is facing away from the aspartate residue to hydrogen bond with an oxygen atom on the γ-phosphate rather than with the aspartate residue (Supplemental Figure 4C). However, following the bond break between the β- and γ-phosphates, Asp166 may exhibit much stronger interactions with the substrate serine which could explain why the substrate then shifts toward the aspartate residue as seen in the PKA and CDK2 transition state mimic structures (Supplemental Figure 4D). Finally, following phosphoryl transfer, these structures suggest that the P-site residue once again flips away from the aspartate residue, which may promote substrate release. Therefore, while the crystal structures reported here do not yield direct evidence of the mechanism of phosphoryl transfer, the structures are consistent with previous computational predictions[20] suggesting a dissociative mechanism where the proton on the substrate residue is accepted late in the reaction.

If a dissociative mechanism does govern phosphoryl transfer, then this may have implications for the findings from these phosphoryl transfer structures. Namely, with a dissociative mechanism it is likely to be the stabilization of the leaving group that dominates the reaction energetics. It is possible that this could alter the requirements of the magnesium ions because of the use of AMP-PNP rather than ATP, and we should be cautious to make conclusions about the mechanism of reaction progression when using an unnatural ligand. However, a dissociative mechanism involves the formation of a metaphosphate transition state, which would be the same whether the nucleotide is ATP or AMP-PNP. Therefore, the energetics of the transition state should not be altered with AMP-PNP, but it is possible that following phosphoryl transfer

AMP-PN may not have the same magnesium requirements as ADP, which could influence magnesium ion binding. However, the similar findings obtained with CDK2 of ADP binding either one or two magnesium ions, with Mg1 being the ion that binds less tightly,[26] support the findings from this study and make it more likely that this does represent a step in reaction progress by protein kinases. Additionally, even if AMP-PN perhaps requires less magnesium ion stabilization thereby promoting the release of one ion, then this would still suggest that Mg1 is likely to be the ion that binds less tightly and is less important for ADP binding.

CONCLUSIONS

The findings presented here provide structural evidence for kinase catalyzed phosphoryl transfer of AMP-PNP. Because phosphoryl transfer occurred slowly in the protein crystals and because both products were captured in the crystal lattice, we were able to characterize a midpoint and end point in the phosphoryl transfer reaction. These structures provide direct evidence of the steps involved in phosphoryl transfer and yield important advancements in our understanding of kinase reaction progression and mechanism. We find that Mg2 is likely the first and last magnesium ion present in the active site, while Mg1 is expelled following phosphoryl transfer which may be an important step that precedes ADP release. This sequence of events also appears to govern phosphoryl transfer in CDK2,[26] and therefore, it may be a general mechanism for phosphoryl transfer progression in protein kinases that utilize two magnesium ions.

ASSOCIATED CONTENT

Supporting Information

The coordinates for the partial phosphoryl transfer structure, 4HPU, and full transfer structure, 4HPT, are available free of charge at http://pubs.acs.org and are available via the RCSB Protein Data Bank. Supporting Information including crystallization statistics, mass spectrometry analysis of the protein crystals, magnesium B-factor ratios from several structures, Western blot of C-subunit phosphorylation of RIIβ with AMP-PNP, and other structural information is also provided. This material is available free of charge via the Internet at http://pubs.acs.org.

AUTHOR INFORMATION

Corresponding Author

staylor@ucsd.edu

Notes

The authors declare no competing financial interest.

ACKNOWLEDGMENTS

The project described was supported by the National Institute of Health Grants GM19301 (S.S.T.) and F31GM099415 (A.C.B.). Additionally, A.C.B. was funded by the Ford Foundation Diversity Fellowship. Additional support was provided by the UCSD Graduate Training Program in Cellular and Molecular Pharmacology through an institutional training grant from the National Institute of General Medical Sciences, T32 GM007752 (J.M.S.), and through support by a Ruth L. Kirschstein National Research Service Award NIH/NCI T32 CA009523 (J.M.S.). We would like to thank Alexandr Kornev and Ping Zhang for helpful input and discussions. We thank the ALS staff for their help with data collection.

REFERENCES

(1) Manning, G.; Whyte, D. B.; Martinez, R.; Hunter, T.; Sudarsanam, S. *Science* **2002**, *298*, 1912.
(2) Taylor, S. S.; Kornev, A. P. *PKA: Prototype for Dynamic Signaling in Time and Space. Quantitative Biology: From Molecular to Cellular Systems*; Wall, M. E., Ed.; CRC Press: Boca Raton, London, New York, 2012; pp 267−298.
(3) Tasken, K.; Skalhegg, B. S.; Tasken, K. A.; Solberg, R.; Knutsen, H. K.; Levy, F. O.; Sandberg, M.; Orstavik, S.; Larsen, T.; Johansen, A. K.; Vang, T.; Schrader, H. P.; Reinton, N. T.; Torgersen, K. M.; Hansson, V.; Jahnsen, T. *Adv. Second Messenger Phosphoprotein Res.* **1997**, *31*, 191.
(4) Johnson, D. A.; Akamine, P.; Radzio-Andzelm, E.; Madhusudan, M.; Taylor, S. S. *Chem. Rev.* **2001**, *101*, 2243.
(5) Kim, C.; Cheng, C. Y.; Saldanha, S. A.; Taylor, S. S. *Cell* **2007**, *130*, 1032.
(6) Knighton, D. R.; Zheng, J. H.; Ten Eyck, L. F.; Ashford, V. A.; Xuong, N. H.; Taylor, S. S.; Sowadski, J. M. *Science* **1991**, *253*, 407.
(7) Taylor, S. S.; Keshwani, M. M.; Steichen, J. M.; Kornev, A. P. *Philos. Trans. R. Soc. London: Ser. B* **2012**, *367*, 2517.
(8) Zheng, J.; Trafny, E. A.; Knighton, D. R.; Xuong, N. H.; Taylor, S. S.; Ten Eyck, L. F.; Sowadski, J. M. *Acta Crystallogr., Sect. D* **1993**, *49*, 362.
(9) Masterson, L. R.; Shi, L.; Metcalfe, E.; Gao, J.; Taylor, S. S.; Veglia, G. *Proc. Natl. Acad. Sci. U.S.A.* **2011**, *108*, 6969.
(10) Armstrong, R. N.; Kondo, H.; Granot, J.; Kaiser, E. T.; Mildvan, A. S. *Biochemistry* **1979**, *18*, 1230.
(11) Grace, M. R.; Walsh, C. T.; Cole, P. A. *Biochemistry* **1997**, *36*, 1874.
(12) Bossemeyer, D.; Engh, R. A.; Kinzel, V.; Ponstingl, H.; Huber, R. *EMBO J.* **1993**, *12*, 849.
(13) Herberg, F. W.; Doyle, M. L.; Cox, S.; Taylor, S. S. *Biochemistry* **1999**, *38*, 6352.
(14) Adams, J. A.; Taylor, S. S. *Protein Sci.* **1993**, *2*, 2177.
(15) Zheng, J.; Knighton, D. R.; ten Eyck, L. F.; Karlsson, R.; Xuong, N.; Taylor, S. S.; Sowadski, J. M. *Biochemistry* **1993**, *32*, 2154.
(16) Shaltiel, S.; Cox, S.; Taylor, S. S. *Proc. Natl. Acad. Sci. U.S.A.* **1998**, *95*, 484.
(17) Shaffer, J.; Adams, J. A. *Biochemistry* **1999**, *38*, 5572.
(18) Cook, P. F.; Neville, M. E., Jr.; Vrana, K. E.; Hartl, F. T.; Roskoski, R., Jr. *Biochemistry* **1982**, *21*, 5794.
(19) Kovalevsky, A. Y.; Johnson, H.; Hanson, B. L.; Waltman, M. J.; Fisher, S. Z.; Taylor, S.; Langan, P. *Acta Crystallogr., Sect. D* **2012**, *68*, 854.
(20) Valiev, M.; Yang, J.; Adams, J. A.; Taylor, S. S.; Weare, J. H. *J. Phys. Chem. B* **2007**, *111*, 13455.
(21) Cheng, Y.; Zhang, Y.; McCammon, J. A. *J. Am. Chem. Soc.* **2005**, *127*, 1553.
(22) Szarek, P.; Dyguda-Kazimierowicz, E.; Tachibana, A.; Sokalski, W. A. *J. Phys. Chem. B* **2008**, *112*, 11819.
(23) Tereshko, V.; Teplova, M.; Brunzelle, J.; Watterson, D. M.; Egli, M. *Nat. Struct. Biol.* **2001**, *8*, 899.
(24) Wu, J.; Tseng, Y. D.; Xu, C. F.; Neubert, T. A.; White, M. F.; Hubbard, S. R. *Nat. Struct. Mol. Biol.* **2008**, *15*, 251.
(25) Bao, Z. Q.; Jacobsen, D. M.; Young, M. A. *Structure* **2011**, *19*, 675.
(26) Jacobsen, D. M.; Bao, Z. Q.; O'Brien, P.; Brooks, C. L., III; Young, M. A. *J. Am. Chem. Soc.* **2012**, *134*, 15357.
(27) Mukherjee, K.; Sharma, M.; Urlaub, H.; Bourenkov, G. P.; Jahn, R.; Sudhof, T. C.; Wahl, M. C. *Cell* **2008**, *133*, 328.
(28) Adams, J. A. *Chem. Rev.* **2001**, *101*, 2271.
(29) Gibbs, C. S.; Zoller, M. J. *J. Biol. Chem.* **1991**, *266*, 8923.
(30) Valiev, M.; Kawai, R.; Adams, J. A.; Weare, J. H. *J. Am. Chem. Soc.* **2003**, *125*, 9926.
(31) Zoller, M. J.; Nelson, N. C.; Taylor, S. S. *J. Biol. Chem.* **1981**, *256*, 10837.
(32) Iyer, G. H.; Garrod, S.; Woods, V. L., Jr.; Taylor, S. S. *J. Mol. Biol.* **2005**, *351*, 1110.

(33) Iyer, G. H.; Moore, M. J.; Taylor, S. S. *J. Biol. Chem.* **2005**, *280*, 8800.
(34) Madhusudan; Akamine, P.; Xuong, N. H.; Taylor, S. S. *Nat. Struct. Biol.* **2002**, *9*, 273.
(35) Olsen, S. R.; Uhler, M. D. *Mol. Endocrinol.* **1991**, *5*, 1246.
(36) Madhusudan; Trafny, E. A.; Xuong, N. H.; Adams, J. A.; Ten Eyck, L. F.; Taylor, S. S.; Sowadski, J. M. *Protein Sci.* **1994**, *3*, 176.
(37) Yount, R. G.; Babcock, D.; Ballantyne, W.; Ojala, D. *Biochemistry* **1971**, *10*, 2484.
(38) Tomaszek, T. A., Jr.; Schuster, S. M. *J. Biol. Chem.* **1986**, *261*, 2264.
(39) Suzuki, Y.; Shimizu, T.; Morii, H.; Tanokura, M. *FEBS Lett.* **1997**, *409*, 29.
(40) Taylor, J. S. *J. Biol. Chem.* **1981**, *256*, 9793.
(41) Herberg, F. W.; Bell, S. M.; Taylor, S. S. *Protein Eng.* **1993**, *6*, 771.
(42) Duronio, R. J.; Jackson-Machelski, E.; Heuckeroth, R. O.; Olins, P. O.; Devine, C. S.; Yonemoto, W.; Slice, L. W.; Taylor, S. S.; Gordon, J. I. *Proc. Natl. Acad. Sci. U.S.A.* **1990**, *87*, 1506.
(43) Bastidas, A. C.; Deal, M. S.; Steichen, J. M.; Keshwani, M. M.; Guo, Y.; Taylor, S. S. *J. Mol. Biol.* **2012**, *422*, 215.
(44) Wu, J.; Yang, J.; Kannan, N.; Madhusudan; Xuong, N. H.; Ten Eyck, L. F.; Taylor, S. S. *Protein Sci.* **2005**, *14*, 2871.
(45) Yang, J.; Ten Eyck, L. F.; Xuong, N. H.; Taylor, S. S. *J. Mol. Biol.* **2004**, *336*, 473.
(46) Battye, T. G.; Kontogiannis, L.; Johnson, O.; Powell, H. R.; Leslie, A. G. *Acta Crystallogr., Sect. D* **2011**, *67*, 271.
(47) McCoy, A. J.; Grosse-Kunstleve, R. W.; Adams, P. D.; Winn, M. D.; Storoni, L. C.; Read, R. J. *J. Appl. Crystallogr.* **2007**, *40*, 658.
(48) Thompson, E. E.; Kornev, A. P.; Kannan, N.; Kim, C.; Ten Eyck, L. F.; Taylor, S. S. *Protein Sci.* **2009**, *18*, 2016.
(49) Acta Crystallogr, D. *Biol Crystallogr* **1994**, *50*, 760.
(50) Emsley, P.; Cowtan, K. *Acta Crystallogr., Sect. D* **2004**, *60*, 2126.
(51) Zhang, P.; Smith-Nguyen, E. V.; Keshwani, M. M.; Deal, M. S.; Kornev, A. P.; Taylor, S. S. *Science* **2012**, *335*, 712.
(52) Brown, S. H.; Wu, J.; Kim, C.; Alberto, K.; Taylor, S. S. *J. Mol. Biol.* **2009**, *393*, 1070.
(53) Khavrutskii, I. V.; Grant, B.; Taylor, S. S.; McCammon, J. A. *Biochemistry* **2009**, *48*, 11532.
(54) Yang, J.; Cron, P.; Good, V. M.; Thompson, V.; Hemmings, B. A.; Barford, D. *Nat. Struct. Biol.* **2002**, *9*, 940.